



Crevice corrosion performance of high-alloy stainless steels and Ni-based alloy in desalination industry

N. Larché*, P. Boillot, P. Dezerville, E. Johansson, J.M. Lardon, D. Thierry

Industeel ArcelorMittal R&D, Le Creusot Research Center, 56 rue Clémenceau B.P.19 71201 Le Creusot Cedex, France, emails: nicolas.larche@institut-corrosion.fr (N.Larché), pauline.boillot@arcelormittal.com (P.Boillot)

Received 28 February 2014; Accepted 16 June 2014

ABSTRACT

Several high alloys are candidate materials for the severe corrosive environment of reverse osmosis desalination plants. In the present study, the crevice corrosion performance of duplex, superduplex, superaustenitic stainless steels, and nickel-based alloy was investigated in natural and chlorinated seawater, at different temperatures. Several crevice configurations were evaluated including flanges assembled with gaskets, bolts mounted with nuts to plates, and the standard CREVCORR-type crevice formers. It was thus possible to illustrate the effect of crevice configuration on the corrosion behavior of the different alloys. The crevice geometry was confirmed to be of major importance in terms of risk for initiating crevice corrosion. In natural seawater (i.e. not chlorinated), the most severe temperature was 30°C, due to high biological activity and high corrosion kinetics. Chlorination at 0.5 ppm increased the risk of localized corrosion but decreased the corrosion propagation rates. In chlorinated seawater, crevice corrosion risk significantly increased with temperature for all tested alloys. For each of the tested configurations, the superaustenitic stainless steel UNS S31266 showed better crevice corrosion resistance than superaustenitic UNS S31254 and S34565, superduplex S32750, and also nickel-based alloy N06625. The present results are part of a three-year Joint Industry Program supported by end-users, engineering companies, and material producers.

Keywords: Stainless steel; Nickel-based alloy; Crevice corrosion; Seawater; Biofilm; Chlorination; Flange; Bolt and nut; Crevice corrosion

1. Introduction

High-alloy stainless steels and nickel-based alloys have been used for a wide range of applications in seawater and chlorinated seawater for more than

25 years. Most corrosion problems in seawater were expected to disappear with the use of these “high-grade” alloys but many failures due to pitting and crevice corrosion appeared in field service conditions [1–3]. In the last decades, the understanding of crevice corrosion has received much attention since it is often

*Corresponding author.

Previously published as part of The International Desalination Association (IDA) World Congress Proceedings, Tianjin 2013

*Presented at the Conference on Desalination for the Environment: Clean Water and Energy
11–15 May 2014, Limassol, Cyprus*

the limiting factor for the use of “high-grade” stainless steels for seawater applications. This has led to the need to better understand the parameters which influence crevice corrosion and to develop laboratory testing methods able to reproduce this type of failure in order to predict long-term behavior of the materials, in conditions close to actual operating conditions. Hence, a lot of field experiences are available today as well as laboratory results, enabling a safer use of these materials in seawater. However, contradictory “corrosion resistance data” can be found in the literature since the actual corrosion risk on high-alloyed stainless steels (e.g. UNS S31254, S32750, N08367, and S31266) and nickel-based alloys (e.g. N06625, N06276, N06022, and N06059) will strongly depend on the exact service conditions (e.g. temperature, chlorination, oxygen content, and flowing conditions), on the metallurgy (e.g. cast or wrought alloys), and on the geometrical configuration of the confined zones in contact with seawater [4,5], as well as surface contamination [6]. Unfortunately, in many literature studies, the actual crevice geometry is often poorly described, making any overall comparison impossible. From this background, it appeared important to better understand the corrosion resistance of high-alloy stainless steels and Ni-based alloys, used under “close to service condition” and detailed crevice configurations.

The main aim of the present study was to get a deeper knowledge on the influence of crevice geometry and service conditions on crevice corrosion and to obtain practical engineering data to help material selection stainless steel and nickel-based alloys in seawater reverse osmosis units. This is performed with

the testing of industrial assemblies (i.e. bolted plates and assembled flanges) together with well-defined standard crevice assemblies, in natural and chlorinated seawater, at different temperatures. The selected crevice assemblies are expected to be the representative of more or less “severe” industrial crevice configurations such as flanges, treaded connections, and plastic contacts inducing confined areas.

2. Experimental

2.1. Material

The composition of the tested alloys is given in Table 1. Both stainless steels and nickel-based alloy were used. The usual PREN formula for stainless steels (i.e. $w\%Cr + 3.3 w\%Mo + 16 w\%N$) might not be applicable to nickel-based alloys, that is why the formula of $PREN_{WNB}$ (i.e. $w\%Cr + 1.5 (w\%Mo + w\%W + w\%Nb) + 30 w\%N$) is also mentioned [7].

2.2. Tested specimens

Three different types of assemblies were used: flanges, bolts and nuts, and CREVCORR crevice formers on plates.

The flanges were machined according to the picture given in Fig. 1. The surface at gasket location is according to ANSI requirements with surface finish of 125–150 microinches of the raised annular surface and continuous spiral groove with 50 groove per inch, 0.06 inch radius on cutting tool.

According to the literature for seawater applications, gasket made of aramid synthetic fibers (Latty®

Table 1
Composition (w%) and PREN of the tested materials per type of crevice enhancing specimens

UNS	Type of specimen	Cr	Ni	Mo	Fe	Cu	N	W	Nb	PREN	$PREN_{WNB}$
S32205	Flange	21.6	5.4	2.9	bal.	0.35	0.18	–	–	34.1	31.4
	Plate	22.4	5.7	3.2	bal.	0.24	0.18	–	–	35.8	32.6
S31254	Plate	20.1	17.8	6.0	bal.	0.72	0.20	–	–	43.1	35.1
N08367	Flange	20.4	23.7	6.2	bal.	0.25	0.22	–	–	44.4	36.3
S32750	Flange	25.0	6.9	4.1	bal.	0.12	0.28	–	–	43.0	39.6
	Plate	25.1	7.0	3.8	bal.	0.13	0.29	–	–	42.3	39.5
S34565	Plate	23.8	17.3	4.4	bal.	0.17	0.46	–	–	45.7	44.2
S31266	Flange	24.3	22.0	5.5	bal.	1.67	0.50	2.0	–	50.5	50.6
	Plate	24.1	22.6	5.6	bal.	1.61	0.46	2.0	–	49.9	49.3
N06625	Flange	22.3	bal.	9.3	2.8	–	–	–	3.37	53.0*	41.3
	Plate	22.1	bal.	8.9	4.6	–	–	–	3.14	51.5*	40.2

Notes: PREN = pitting resistant equivalent number = $w\%Cr + 3.3 w\%Mo + 16 w\%N$; $PREN_{WNB} = w\%Cr + 1.5 (w\%Mo + w\%W + w\%Nb) + 30 w\%N$ [7].

*PREN formula not adapted to nickel-based alloy.

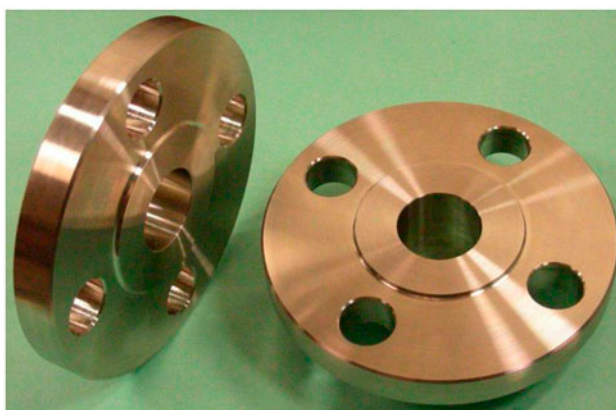


Fig. 1. Photograph of the selected flange.

gold32) was selected for the crevice corrosion tests of the flanges [6–8]. Regarding the flange design, the recommendation from the gasket manufacturer was to apply a final torque of 33 Nm on the 4 bolts. The estimated gasket pressure was 35 N/mm. The importance of geometry under crevice formers on crevice corrosion has been shown in several studies [9,10]; as a result, it appeared important to precisely characterize the surfaces in contact with gaskets. The striated surface for gasket location was thus analyzed with a profilometer WYCO NT1100 from Veeco. The results reveal the spiral grooves with height of about 200 μm and space between 2 peaks of about 500 μm . In principle, the smaller the gaps under crevice formers, the higher the susceptibility to crevice corrosion. Thus, striated surfaces are expected to improve crevice corrosion resistance.

Standard M8 bolt and nuts (i.e. Ø 8 mm, length = 4 cm, bolt: VH DIN933, nut: EHU DIN 934) were used. They were tightened on 150×100 mm plates made of the same material, leading to an anode-to-cathode ratio above 1:60. A picture of the assembly is given on Fig. 2. The selected torque on the M8 bolt and nut systems was 9.5 Nm. It corresponds to the recommended torque for M8 class A stainless steel. The calculated tensile force is then 5,000 N in the bolt, and the calculated pressure is about 21 N/mm below head bolt and below nut [11]. Although some tested materials could support higher torques, and the same torque was used for all the tested alloys in order to provide comparable results from the same crevice geometry. The average roughness of the plates was $3.5 \pm 0.3 \mu\text{m}$.

The crevice assembly used for this study is based on the CREVCORR crevice assembly [12] with the following characteristics: Crevice formers were made of polyvinylidene fluoride (PVDF), and all fasteners were made of titanium grade 2 and electrically isolated

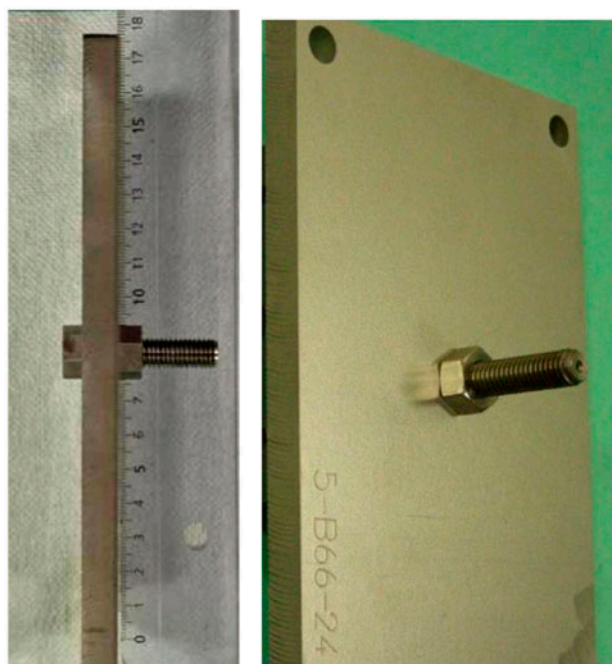


Fig. 2. Photographs of the bolt and nut assembly.

from the tested specimen. According to the standard “CREVCORR” testing method, the crevice former should be tightened to the test specimens with a force of about 900 N (i.e. pressure of about 3 N/mm), which corresponds to a torque of 3 Nm with the crevice assembly that was used [12]. However, for the present investigation, the CREVCORR crevice assembly was adapted to allow gasket pressures up to 20 N/mm in order to get more severe crevice configuration which may be encountered in actual applications. Photographs of the crevice assembly are shown in Fig. 3. All the PVDF gaskets were polished with 600-grit paper to ensure a similar surface finish on crevice formers. The crevice formers were all mounted on specimens in immersion in seawater in order to get seawater under the crevice formers from the beginning of the exposure. The anode (surface under crevice formers)-to-cathode (surface in contact with bulk environment) ratio was 1:30 (plate size: 100×150 mm). The tested plates are similar to those which are used for “bolt and nut” specimens, with the similar average roughness of $3.5 \pm 0.3 \mu\text{m}$.

2.3. Conditions of exposure

The exposures were all performed in natural seawater. All the tested specimens were exposed at 20, 30, and 50 °C in non-chlorinated and/or chlorinated seawater with at least three replicates per condition.

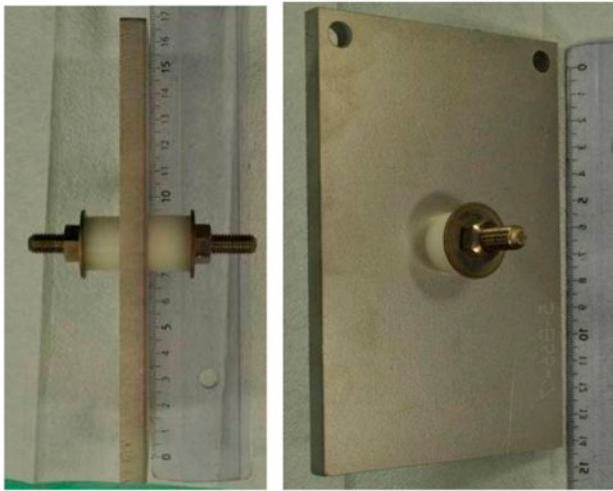


Fig. 3. Photographs of the tested “CREVCORR-type” assembly.

The natural seawater was directly and continuously taken from the open sea in the Bay of Brest (Atlantic ocean, France) with average salinity of 35‰ and pH 8.1 ± 0.1 . For all exposure conditions, the dissolved oxygen content was at the saturated value for a given temperature of the seawater (i.e. continuous renewal of stirred natural seawater, opened to atmosphere).

Flanges were exposed in seawater loops allowing a seawater flow rate at about 1 m/s. The other specimens (i.e. CREVCORR-type as well as bolt and nut assemblies) were exposed in regulated seawater tanks with a renewal rate of 300 L/d (i.e. one complete renewal of the seawater every two days).

Dynamic cathodic polarization curves were performed directly in the exposure tanks, on some specimens exposed 3 months without crevice former. For this purpose, a Gamry ref600 potentiostat was used with scan rate of 0.167 mV/s, starting for the open-circuit potential. These measurements allowed to compare cathodic reduction efficiency between different alloys and between different service conditions (i.e. effect of chlorination).

3. Results

3.1. CREVCORR-type assemblies

All the results from CREVCORR-type assemblies are summarized in Fig. 4. Except in chlorinated seawater at 50°C, only the UNS S31266 resisted crevice corrosion for all the tested conditions of exposure. In chlorinated seawater at 30°C, both UNS S31266 and UNS S34565 showed better corrosion resistance than UNS N06625. In this case, 5 replicates allowed draw-

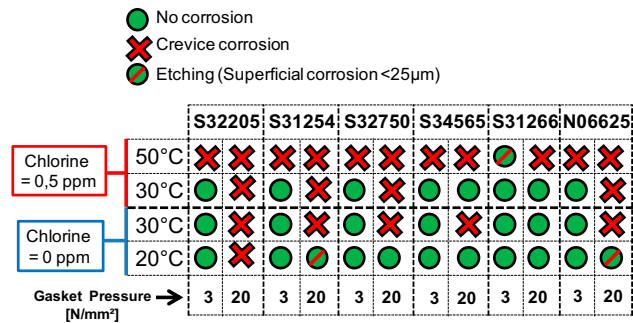


Fig. 4. Summary of results from CREVCORR-type assemblies in natural seawater. Ra of tested plates = 3.5 μm.

ing this conclusion. From all the tested conditions of exposure, the alloys can be ranked as followed: UNS S32205 < S31254–S32750–N06625 < S34565 < S31266. A significant difference was found in terms of crevice corrosion initiation and propagation between exposures at 20 and 30°C, with obvious lower propagation rates at 20°C. The chlorination globally led to a decrease in the crevice corrosion propagation rates in comparison with natural seawater as it is illustrated in Fig. 5.

3.2. Bolt and nuts assemblies

The corrosion results are summarized in Fig. 6 for bolted assemblies after three months of exposure. Only the less alloyed UNS S32205 bolted assembly showed crevice corrosion at 20 and 30°C in natural seawater and at 30°C in chlorinated seawater. Under this condition of exposure at 30°C in natural seawater, only the nut corroded on plane surface in contact with

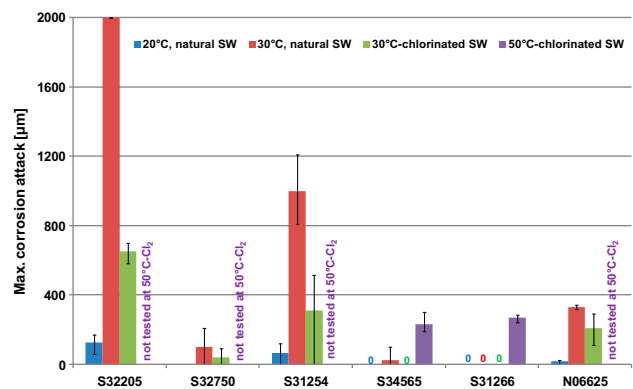


Fig. 5. Crevice corrosion propagation from CREVCORR assemblies (20 N/mm, Ra = 3.5 μm) in natural seawater (SW) at 20 and 30°C and in chlorinated seawater at 30 and 50°C.

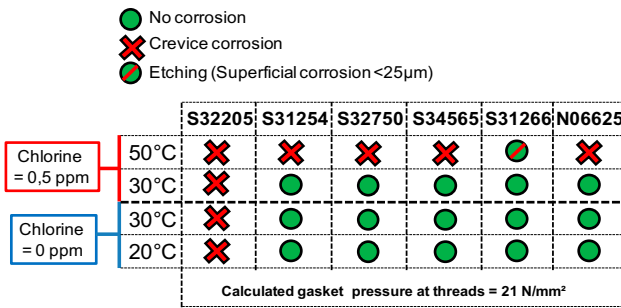


Fig. 6. Summary of results from bolt and nuts assemblies in natural seawater.

the plate, with maximum corrosion attack of 101 µm after 3 months of exposure. Below the nut, the plate showed only etching (i.e. superficial corrosion below 25 µm). In chlorinated seawater at 30°C, a severe propagation rate was observed both in the bolt and in the nut, at the threads. Under the conditions 50°C in chlorinated seawater, a potential plateau was measured of about 450–550 mV/SCE for non-corroded Ni-based alloys and 650–690 mV/SCE for non-corroded stainless steel grades. Crevice corrosion initiated on UNS S31254, S32750, S34565, S31266, and N06625 with a rather low propagation. In all cases, the corrosion initiated and propagated on plane surfaces below the nut and/or the bolt head. The maximum crevice corrosion attacks are indicated in Fig. 7. Only etching (i.e. <25 µm) was noticed on bolted assemblies made of UNS S31266.

3.3. Flanges

Flanges made of UNS S32205, S32750, N08367, S31266, and N06625 were exposed for 3 months in both natural and chlorinated seawater loop. In natural seawater, the corrosion resistance of the flanges was evaluated at 30°C, and in chlorinated seawater, both 30 and 50°C were evaluated (except UNS S32205 which was not evaluated in chlorinated seawater at 50°C). After exposure, all the specimens were visually inspected, and results are summarized in Fig. 8. It shows that both in natural and chlorinated seawater at 30°C, only the less alloyed UNS S32205 flanges severely creviced, while all the other tested alloys resisted crevice corrosion (i.e. N08637, S32750, S31266, and N06625). In chlorinated seawater at 50°C, flanges made of N08637 and UNS S32750 severely creviced and also UNS N06625 to a lesser extent. In this severe condition, only the stainless steel UNS S31266 resisted crevice corrosion. Photographs of creviced specimens after 3-month exposure in chlorinated seawater at

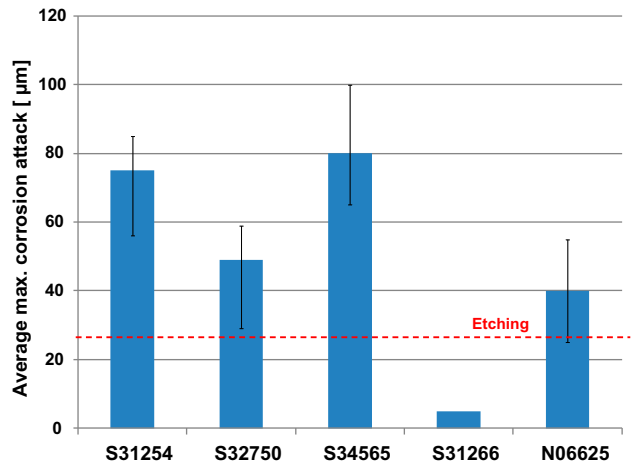


Fig. 7. Average maximum crevice corrosion depth for bolt and nut-type assemblies exposed 3 months in 0.5 ppm-chlorinated seawater at 50°C. The corrosion always initiated and propagated on plane surface below nuts and/or bolt head. Five replicates per grade were tested.

50°C are given in Figs. 9 and 10. A photograph of UNS S31266 flange exposed under similar conditions is given in Fig. 11.

4. Effects of chlorination, temperature, crevice geometry, and composition

4.1. Effects of chlorination and temperature

Globally, it was confirmed that chlorination increases the risk of crevice corrosion initiation and that biofouling (i.e. natural seawater without chlorination) increases the rate of crevice corrosion propagation once initiated. The differences in terms of crevice corrosion propagation rates are illustrated in Fig. 12, showing that the effect of chlorination is more pronounced on stainless steels (i.e. UNS S32205, S31254, and S32750) than on the Ni-based

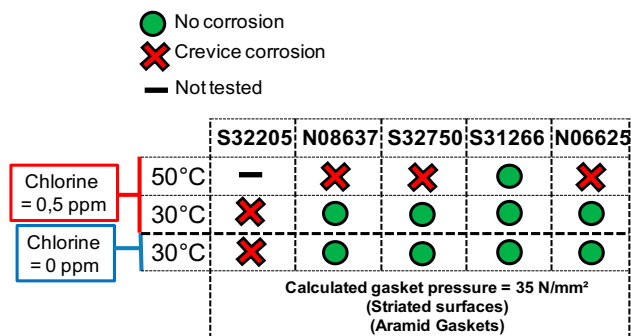


Fig. 8. Summary of results from flanges tested in natural seawater loops.

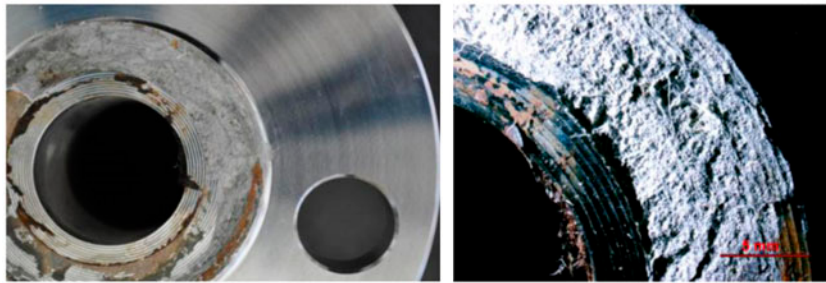


Fig. 9. Photographs of corroded UNS S32750 flanges (striated surface + aramid gasket) after 3 months in chlorinated seawater (0.5 ppm) at 50°C.

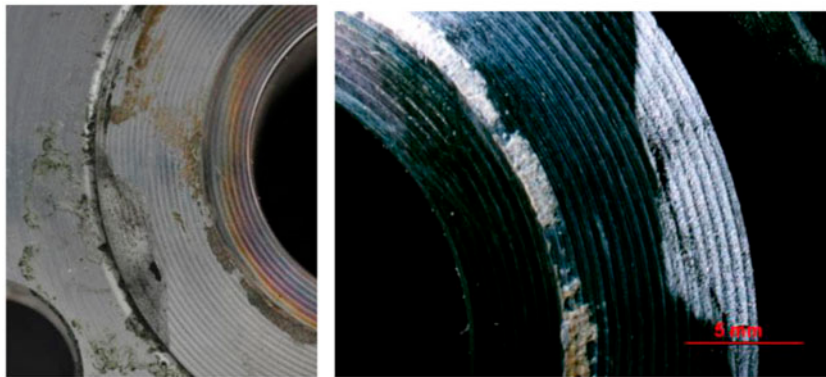


Fig. 10. Photographs of corroded UNS N06625 flanges (striated surface + aramid gasket) after 3 months in chlorinated seawater (0.5 ppm) at 50°C.

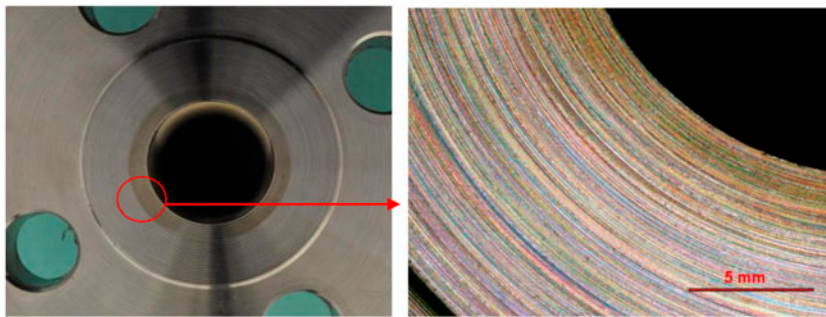


Fig. 11. Photograph of an UNS S31266 flange (striated surface + aramid gasket) after 3 months in chlorinated seawater (0.5 ppm) at 50°C (no corrosion).

alloy UNS N06625. This is probably due to the fact that the potential difference in chlorinated and non-chlorinated seawater is less important for Ni-based alloy than for stainless steels (i.e. potential difference of about 300 mV for stainless steels and less than 100 mV for Ni-based alloys), as summarized in Table 2.

In order to check that the cathodic reduction of oxygen was similar on stainless steel and Ni-based alloy, cathodic polarization curves were performed on

UNS S32750 and N06625 in natural and chlorinated seawater. Results are given in Fig. 13, confirming a similar behavior for both alloys in terms of cathodic reduction reactions. The global higher corrosion rates in non-chlorinated seawater are due to better cathodic reduction efficiency on biofilmed specimens (i.e. exposed in natural seawater with no chlorination) in comparison with specimens in chlorinated seawater. This phenomenon was also clearly shown in previous

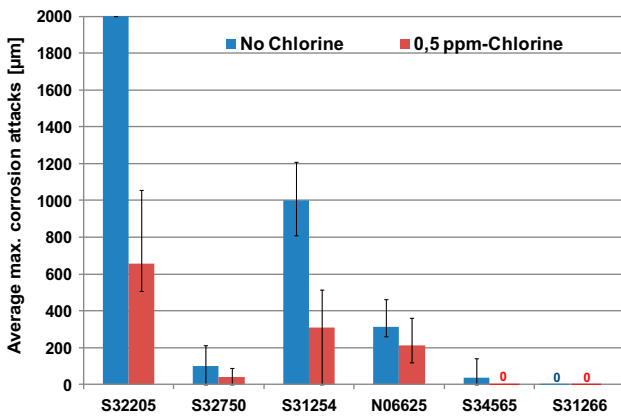


Fig. 12. Crevice corrosion after 3 months in natural and chlorinated seawater at 30 °C with CREVCORR-type assembly (20 N/mm, Ra = 3.5 µm).

studies [13,14]. In chlorinated seawater, the crevice corrosion risk is increased with increasing temperatures, which is in good line with the literature [4,15,16]. In the present study, all the tested alloys which resisted crevice corrosion in chlorinated seawater at 30 °C initiated crevice corrosion in chlorinated seawater at 50 °C, as shown in Fig. 14.

Both the chlorination and the temperature had a direct effect on the electrochemical potentials, which might be the main explanation for the observed differences in terms of localized corrosion results. However, no significant difference in potential evolution was found between natural seawater at 20 and 30 °C (i.e. both around +300 mV/SCE), while significant corrosion results were noticed for materials such as superduplex stainless steels. Similar observations can be done in chlorinated seawater when comparing 30 and 50 °C. In this case, the kinetics of the corrosion initiation and propagation have been significantly influenced by the temperature only. It is recalled that in non-chlorinated seawater, the Ni-based alloy showed similar OCP than stainless steels, while in chlorinated seawater, the OCP of Ni-based alloy was from 200 to 300 mV lower.

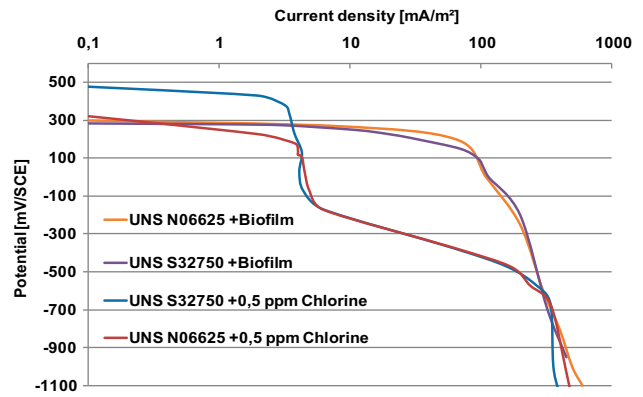


Fig. 13. Dynamic cathodic polarization curves of UNS S32750 and N06625 in natural and chlorinated (0.5 ppm) seawater at 30 °C.

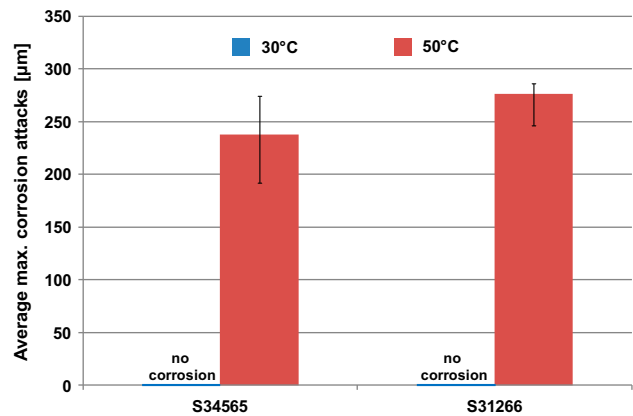


Fig. 14. Crevice corrosion after 3 months in chlorinated seawater at 30 and 50 °C with CREVCORR-type assembly at the highest torque 20 N/mm (Ra = 3.5 µm).

4.2. Effect of crevice geometry

In terms of crevice corrosion resistance, obvious differences were found between aramid fiber and PVDF gaskets, with obviously better corrosion resistance with the use of aramid fiber gaskets. One of the main differences between the two gaskets is the

Table 2
Averaged stabilized open-circuit potentials of non-corroded alloys in natural seawater

	Natural seawater 30 °C [mV/SCE]	0.5 ppm-chlorinated seawater 30 °C [mV/SCE]	0.5 ppm-chlorinated seawater 50 °C [mV/SCE]
S31254			
S32750	+280 to +330	+540 to +620	+570 to +650
S31266			
N06625	+260 to +310	+330 to +360	+330 to +380

mechanical properties: Aramid gasket is compressible (i.e. soft), while PVDF reveals high mechanical properties (i.e. hard). Thus, the crevice geometry will obviously be different with the use of the two types of gasket, leading to different crevice corrosion results. However, in the case of aramid gaskets, the crevice corrosion tests were performed on flanges with striated surfaces, while PVDF gaskets were applied on smooth surfaces. Striated surface leads to rougher surfaces below gasket, which is also known to be beneficial for crevice corrosion resistance. Thus, some additional exposures in natural seawater at 30°C were performed to assess the actual effect of each parameter, namely striated surface and nature of the gasket. PVDF and aramid gasket were both applied on striated and non-striated surfaces of UNS S32750. Results are summarized in Table 3. It shows that both striated surface and aramid gasket are beneficial for crevice corrosion resistance. The differences between aramid fiber gasket and PVDF gaskets used at the same gasket pressure of 20 N/mm are illustrated in Fig. 15. It shows that under similar configuration, crevice corrosion initiated with PVDF gasket, and no corrosion occurred with aramid fiber gasket. The beneficial effect of aramid fiber gasket was also shown in the literature [6]. It can be noticed that with the use of PVDF gasket, no crevice corrosion initiated on striated surface (i.e. rougher surface) in natural seawater at 30°C. It probably allowed easier buffering of the confined seawater below the gasket. This effect of “crevice gap” on crevice corrosion is confirmed in the literature from Oldfield et al. investigations [16]. Such results allow to better understand the beneficial effect of striated surfaces on crevice corrosion resistance. The comparison of crevice corrosion results between the flange testing and the CREVCORR-type testing at 20 N/mm is given in Table 4. It confirms the higher severity of CREVCORR-type assemblies when used at gasket pressure of 20 N/mm. This result appears interesting since it shows that this “well-controlled” standard CREVCORR-type assembly can be used to simulate a critical severe application.

Table 3

Crevice Corrosion results from 2-month exposure of UNS S32750 with different gaskets (pressure = 20 N/mm) and different surface finish in natural seawater at 30°C

	PVDF	Aramid fiber
Striated surface	No corrosion	No corrosion
Plane surface	Crevice corrosion	No corrosion

The results from flanges tested in a full-scale loop showed excellent correlation with the flanges tested with a controlled and adapted CREVCORR-type assembly. This was also true for the alloy UNS S32205 which showed crevice corrosion under these configurations. For this alloy, similar corrosion rates were found in the flanged seawater loop and in adapted CREVCORR-type assembly using similar gasket (i.e. aramid fiber). This result appears very interesting for crevice corrosion testing because it seems possible to simulate any crevice configuration with a “simple” standard setup, regarding that the following parameters are respected: nature and pressure of the gasket as well as surface finish of the tested specimen.

The tested “bolt and nuts” specimens clearly induced a less severe crevice configuration compared to CREVCORR-type assembly involving a 20 N/mm pressure, which could be surprising. To better understand this phenomenon, the main differences between the two configurations are summarized in Table 5. Regarding the nature of the contacts, Grolleau et al. showed that metal/metal contacts were less severe than GRP/Metal contacts but more severe than aramid fiber contact [6]. In the present investigation, PDVF/metal contacts were clearly shown to be more severe than aramid fiber/metal. This is in good line with the obtained results. Another explanation could be related to the geometry of the confined zones. In the case of M8 bolt and nuts, the maximum distance below contact is at 0.7 mm from the bulk seawater while the maximum distance below contact is at 3.5 mm for the CREVCORR gasket. Maybe the proximity to the bulk allows a “buffering” of the solution below contacts, leading to better crevice corrosion resistance. Also at the initial stage of corrosion, the crevice will be rapidly opened to the bulk, allowing expected fast repassivation. If this hypothesis is true, bolt and nuts with higher dimensions would not show the same crevice corrosion resistance. Also another hypothesis to explain this result could be the difficulty to precisely estimate the actual pressure at threaded connection from theoretical calculations.

4.3. Effect of alloy composition

The present investigation does not allow evaluating the individual effect of each alloying element on the localized corrosion resistance of materials. However, it allows comparing the global corrosion resistance of the tested alloys, considering their actual chemical composition. For stainless steels, the crevice corrosion results leads globally to this ranking in

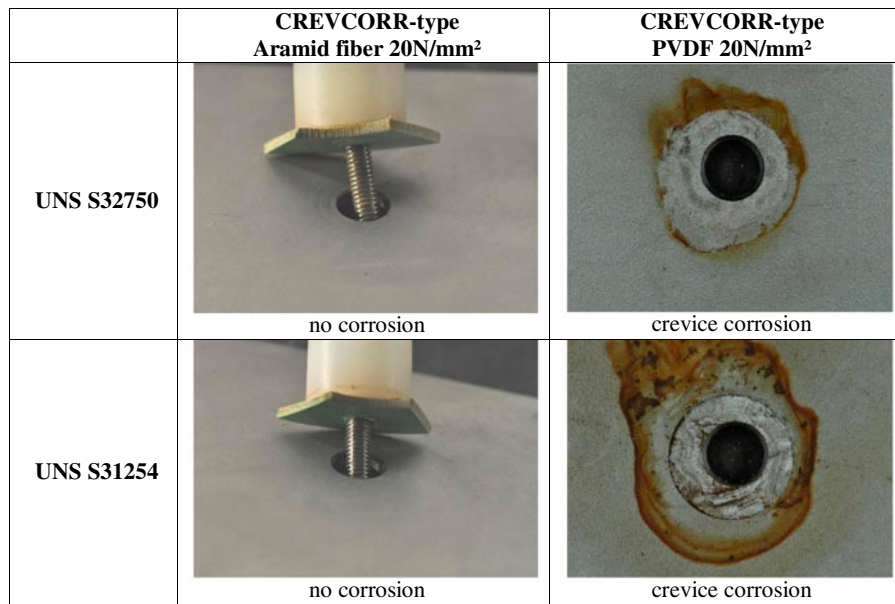


Fig. 15. Crevice Corrosion results from 2 month exposure of UNS S32750 and UNS S31254 with different gaskets at the same pressure (20 N/mm) on smooth surface (Ra = 3.5 μm).

Table 4

Comparison of crevice corrosion results between flange testing and CREVCORR testing in chlorinated seawater at 0.5 ppm chlorine

Alloy	Flange-Aramid 35 N/mm ² on striated surface		CREVCORR-PVDF 20 N/mm ² on smooth Ra 3,5 μm	
	30°C	50°C	30°C	50°C
S32205	✗	✗	✗	✗
S32750	●	✗	✗	✗
N08637	●	✗	✗	✗
S31266	●	●	●	✗
N06625	●	✗	✗	✗

● No corrosion ✗ Crevice Corrosion

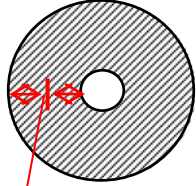

terms of initiation: UNS S33205 < S31254–S32750 < S34565 < S31266.

Moreover, under plate geometry and at closed PREN values, the UNS S32750 showed better results than S31254 in terms of propagation and except the

potentially beneficial differences in microstructure (duplex vs. austenitic, respectively) and nitrogen content (0.29_w% vs. 0.20_w%, respectively); the main parameter was a higher chromium content for superduplex (25_w% vs. 20_w%, respectively). These results

Table 5

Difference of contact geometry between CREVCORR gasket and bolt and nut

	CREVCORR	Bolt&Nut
Nature	PVDF/Metal	Metal/Metal
Pressure	20 N/mm ² (measured)	21N/mm ² (calculated)
Area below gasket	 <p>Max distance to the bulk = 3.5 mm</p>	 <p>= Max. pressure</p> <p>Max distance to the bulk = 0.7 mm</p>
Load	Constant	Possible local relax

may point out the importance of chromium content in the crevice corrosion resistance in seawater and the issue related to the widely used PREN, already mentioned in previous study [4]. Further investigations are needed to confirm this result.

When comparing with the tested nickel-based alloy, it is interesting to notice that for all the tested configurations, the UNS N06625 was less corrosion resistant than S31266 and sometimes less corrosion resistant than UNS S34565. This comparative result was already shown elsewhere between N06625 and S31266 [8]. However, even if corrosion rates were very low, the alloy S31266 is also susceptible to crevice corrosion in the most severe tested conditions (e.g. chlorinated seawater at 50°C with tight crevice geometry at 20 N/mm).

All these results confirm the good correlation between $PREN_{WNb}$ -based ranking of alloys and localized corrosion resistance in natural and chlorinated seawater when comparing stainless steels and nickel-based alloys.

5. Conclusions

Reverse osmosis desalination is a demanding application in terms of corrosion risks, which requires a careful material selection. High-alloy stainless steels and Ni-based alloys may appear as good candidate material, and the corrosion risk will highly depend on the actual service conditions and the involved crevice configurations. In the present study, the influence of temperature and chlorination on the corrosion resistance of several high alloys was investigated. Several crevice configurations were evaluated including flanges, bolts and nuts on plates, and the standard CREVCORR-type crevice

formers. It was thus possible to emphasize the effect of crevice configuration on the results, and the crevice geometry was clearly confirmed to be of major importance in terms of risk for initiating crevice corrosion. In natural seawater (i.e. not chlorinated), the most severe temperature in seawater was 30°C, due to the high biological activity and high corrosion kinetics. The effect of chlorination at 0.5 ppm was to increase the risk of localized corrosion, but it also decreased the corrosion propagation rates. In chlorinated seawater, crevice corrosion risk significantly increased with the temperature for all the tested alloys. For all the tested configurations, the ranking of high-alloy stainless steels was established under the tested conditions and compared with a nickel-based alloy. In the most severe conditions tested in the study in terms of crevice geometry, temperature, and chlorination treatment, the superaustenitic stainless steel UNS S31266 showed better crevice corrosion resistance than superaustenitic UNS S31254, S34565, superduplex S32750, and also nickel-based alloy N06625. However, it should be underlined that the present study was performed on hot-rolled plates, and that corrosion results are susceptible to be different if alloys present a different metallurgy, for instance, in the case of cast massive equipment.

Comparing crevice severity in terms of geometry, at the same gasket pressure, aramid fiber gaskets were significantly less severe than PVDF ones. Moreover, striated surfaces led to less severe crevice configuration. Finally, bolt and nut configuration (M8 size) was less severe than CREVCORR-type assembly (PVDF, 20 N/mm). With the striated surface and aramid fiber gasket, all the tested alloys with PREN above 42 (UNS S31254, N08367, S32750, S34565, S31266, and N06625) resisted crevice corrosion up to 30°C in 0.5 ppm-

chlorinated seawater, while most of them showed crevice corrosion with PVDF gaskets (i.e. CREVCORR-type assembly). The only flange (using the aramid fiber gasket and striated surface) showing a high susceptibility to crevice corrosion in natural seawater is UNS S32205. At fixed surface roughness, gasket pressure has obvious effect on the crevice corrosion initiation. This investigation showed that it is possible to simulate the actual flange crevice geometry using an adapted CREVCORR-type assembly. Very good correlation was found, in terms of both corrosion initiation and propagation rates.

Acknowledgment

This publication was inspired by the results of joint industrial project managed by the French Corrosion Institute. The following companies are acknowledged for their financial and technical participations to this joint industrial project: Eramet-Aubert & Duval (Jean-Marc Lardon), DCNS (Valérie Debout), DGA (Jérôme Blanc and Jean-Pierre Pautasso), Industeel-ArcelorMittal (Pauline Boillot and Jérôme Peultier), Outokumpu Stainless (Elisabeth Johansson and Rachel Pettersson), Swagelok (Gerhard Schiroky, Roland Kvaternik and Renaud Morla), Total E&P (Thierry Cassagne), and Veolia Water (Philippe Dézerville).

References

- [1] O. Strandmyr, O. Hagerup, Field Experience with Stainless Steel Materials in Seawater Systems, Corrosion'98, Houston, NACE, paper N°. 707, 1998.
- [2] T. Havn, Material Engineering and Fabrication Experiences, Corrosion, NACE paper N°56, 1995.
- [3] R. Johnsen, North Sea Experience with the Use of Stainless Steel in Seawater Applications, EFC Publication 10, The Institute of Materials, 1993.
- [4] N. Larché, D. Thierry, V. Debout, T. Cassagne, J. Peultier, E. Johansson, C. Tavel-Condât, Crevice Corrosion of Duplex Stainless Steels in Natural and Chlorinated Seawater, Duplex World 2010, 11–13 October, 2010.
- [5] H. Yakuwa, M. Miyasaka, K. Sugiyama, Evaluation of Crevice Corrosion Resistance of Duplex and Super duplex Stainless Steels for Seawater Pumps, Corrosion, NACE paper N°09194, 2009.
- [6] A.M. Grolleau, H. Le Guyader, V. Debout, Prediction of Service Life of Nickel Based Alloys N06625 and N06059 and Super Austenitic Stainless Steel S31266 in Seawater using In-House Crevice Corrosion Tests, Nace corrosion, paper N°09192, 2009.
- [7] S.A. McCoy, B.C. Puckett, E.L. Hibner, High Performance Age-Hardenable Nickel Alloys Solve Problems in Sour Oil and Gas Service, Stainless Steel World 14, Houston, TX, 2002, pp. 48–52.
- [8] R. Francis, Factors Affecting Gasket Selection for Stainless Steels in Seawater, Corrosion, Nace paper N°07262, 2007.
- [9] J.W. Oldfield, T.S. Lee, R.M. Kain, Mater. Perf. 23(7) (1984) 9–15.
- [10] T. Rogne, J.M. Drugli, Crevice Corrosion Testing of Stainless Steels, Test Methods and Effect of Crevice Geometry, Stainless Steel World, The Hague, 1999.
- [11] J. Guillot, Modélisation et Calcul des Assemblages Vissés—Généralités (Modelling and Calculation of Screw-mount Assemblies—Generalities), Technique de l'Ingénieur, BM 5 560.
- [12] B. Espelid, Development of a New Crevice Corrosion Qualification Test for Stainless Steels, Stainless Steel World, Maastricht, 2003.
- [13] E. Bardal, R. Johnsen, P.O. Gartland, Corrosion, 40 (1984) 12.
- [14] R. Francis, Coupling of superduplex stainless steel and cast nickel-aluminium bronze in sea water, Br. Corros. J. 34(2) (1999) 139–144.
- [15] G. Nyström, S. Henrikson, Investigation of the Corrosion Resistance of a New High Alloy Duplex Stainless steel in Chlorinated and Unchlorinated Seawater, 11th Scandinavian Corrosion Congress, Paper N. F-14, 1989.
- [16] B. Wallen, S. Henrikson, Effect of Chlorination on Stainless Steels in Seawater, NACE Corrosion '88 paper N. 403, 1988.